Title: The phytosiderophore efflux transporter TOM2 is involved in metal transport in rice

Author: Tomoko Nozoye, Seiji Nagasaka, Takanori Kobayashi, Yuki Sato, Nobuyuki Uozumi, Hiromi Nakanish and Naoko K. Nishizawa

Manuscript Title:	The phytosiderophore efflux transporter TOM2 is involved in metal transport in rice
Manuscript No:	JBC/2014/635193 [R2]
Manuscript Type:	Regular Paper
Date Submitted by the Author:	23 Aug 2015
Complete List of Authors:	Tomoko Nozoye, Seiji Nagasaka, Takanori Kobayashi, Yuki Sato, Nobuyuki Uozumi, Hiromi Nakanish, and Naoko K. Nishizawa
Keywords:	iron; nutrition; plant molecular biology; plant physiology; transporter

The phytosiderophore efflux transporter TOM2 is involved in metal transport in rice*

Tomoko Nozoye[1], Seiji Nagasaka[1], Takanori Kobayashi[2], Yuki Sato[3], Nobuyuki Uozumi[3], Hiromi Nakanishi[1], Naoko K. Nishizawa[1,2]

[1]From Department of Global Agricultural Sciences, Graduate School of Agricultural and Life Sciences, The University of Tokyo, 1-1-1 Yayoi, Bunkyo-ku, Tokyo 113-8657 Japan,
[2]Research Institute for Bioresources and Biotechnology, Ishikawa Prefectural University, Nonoichi, Ishikawa 921-8836, Japan
[3]Department of Biomolecular Engineering, Graduate School of Engineering, Tohoku University, 6-6-7 Aobayama, Sendai 980-8579, Japan,
*Running title: *TOM2 is a DMA efflux transporter crucial for plant growth*
To whom correspondence should be addressed: Naoko K. Nishizawa, 1-1-1 Yayoi, Bunkyo-ku, Tokyo 113-8657, Japan. Fax: 81-3-5841-7514; E-mail: annaoko@mail.ecc.u-tokyo.ac.jp

Keywords: iron; nutrition; plant molecular biology; plant physiology; transporter

Background: Phytosiderophores are important metal chelators for graminaceous plants.
Results: Repression of *TOM2* causes severe growth defects.
Conclusion: TOM2 is a crucial efflux transporter of phytosiderophores.
Significance: TOM2 may enhance crop yield and nutritional quality

ABSTRACT

Iron (Fe) is an essential metal element for all living organisms. Graminaceous plants produce and secrete mugineic acid family phytosiderophores from their roots to acquire Fe in the soil. Phytosiderophores chelate and solubilize insoluble Fe hydroxide in the soil. Subsequently, plants take up Fe-phytosiderophore complexes through specific transporters on the root cell membrane. Phytosiderophores are also thought to be important for the internal transport of various transition metals including Fe. In the present study, we analyzed TOM2 and TOM3, rice homologs of transporter of mugineic acid family phytosiderophores 1 (TOM1), a crucial efflux transporter directly involved in phytosiderophore secretion into the soil. Transgenic rice analysis using promoter-β-glucuronidase (GUS) revealed that *TOM2* was expressed in tissues involved in metal translocation, while *TOM3* was expressed only in restricted parts of the plant. Strong *TOM2* expression was observed in developing tissues during seed maturation and germination, while *TOM3* expression was weak during seed maturation. Transgenic rice in which *TOM2* expression was repressed by RNA interference showed growth defects compared to non-transformants and *TOM3*-repressed rice. *Xenopus laevis* oocytes expressing *TOM2* released ^{14}C-labeled deoxymugineic acid (DMA), the initial phytosiderophore compound in the biosynthetic pathway in rice. In onion epidermal and rice root cells, the TOM2–GFP fusion protein localized to the cell membrane, indicating that the TOM2 protein is a transporter for phytosiderophore efflux to the cell exterior. Our results indicate that TOM2 is involved in the internal transport of DMA, which is required for normal plant growth.

INTRODUCTION

Iron (Fe) is essential for all living organisms, including humans and plants. In plants, Fe is necessary for growth and is required for various cellular activities ranging from photosynthesis to respiration. Under aerobic conditions, Fe is oxidized to Fe hydroxide [$Fe(OH)_3$], which is poorly soluble in water. Thus, although mineral

soils contain 6% Fe by weight, most of it is not available to plants. This phenomenon is exacerbated in high pH soils, including calcareous soils, constituting a major problem for crop production. Moreover, Fe deficiency leads to leaf chlorosis, poor yields, and decreased nutritional quality. Fe uptake in humans is ultimately dependent on the Fe that plants take up from the soil. Therefore, increasing the efficiency of Fe uptake in food plants could have a dramatic, positive impact on both crop productivity and human health.

To acquire Fe, higher plants have two strategies for the uptake of oxidized Fe(III) from the rhizosphere (1). All higher plants, except graminaceous plants, take up iron using ferric-chelate reductases to reduce ferric iron to Fe(II), which is then absorbed by ferrous iron transporters (2–4). Alternatively, graminaceous plants, including important staple crops such as rice, wheat, and barley, secrete natural Fe chelators called mugineic acid family phytosiderophores (MAs) from their roots (5). These MAs have six coordination sites (three –COOH, two –NH, and one –OH) that bind to Fe and are thought to form octahedral Fe(III) complexes, which are soluble (6). The secreted MAs chelate and solubilize gelatinous $Fe(OH)_3$ in the soil, forming Fe(III)–MAs complexes that are absorbed into root cells through the Fe(III)–MAs transporters called yellow stripe 1 (YS1)/YS1-like (YSL) transporters, which localize to the root cell membrane (7, 8). The biosynthetic pathway for MAs in graminaceous plants has been elucidated (9, 10). *S*-adenosyl-L-methionine (SAM), the precursor of MAs, is converted to 2´-deoxymugineic acid (DMA) via four sequential steps catalyzed by SAM synthetase (SAMS), nicotianamine synthase (NAS), nicotianamine aminotransferase (NAAT), and deoxymugineic acid synthase (DMAS) (9–13). Whereas rice and maize secrete DMA, other species, including barley and rye, further hydroxylate DMA to other MAs. The production and secretion of MAs markedly increase in response to Fe deficiency. The secretion of MAs in barley follows a distinct diurnal rhythm with a peak just after sunrise or initial illumination (14, 15). MAs are thought to be specific to graminaceous plants. On the other hand, nicotianamine (NA), an intermediate in MAs biosynthesis and a structural analog of MAs, is produced in all plants examined thus far, including non-graminaceous plants such as *Arabidopsis*, tomato, and tobacco (16–20).

In the plant body, free Fe^{2+} is toxic. Therefore, Fe transport requires complex formation with some component. MAs and NA are also essential for the translocation of metal nutrients inside the body of the plant. MAs and NA are able to chelate not only Fe but also various transition metals such as zinc (Zn), manganese (Mn), and copper (Cu) (16, 17, 21–23). These metals are micronutrients and are important for plant development because they are necessary for the activities and structures of various proteins. Because MAs have been identified in the xylem and phloem of rice and barley, they are also suggested to play an important role in the long-distance transport of metals in graminaceous plants (23–26). NA has been suggested to play an essential role in metal translocation and accumulation in developing seeds based on an analysis of the tomato *chloronerva* mutant (19) and NA-deficient transgenic tobacco (*Nicotiana tabacum*) plants (20). In addition, MAs and NA were suggested to be involved in metal transport during rice seed germination based on results from physiological analyses using *YSL* knockdown rice lines, and expression analyses using promoter-ß-glucuronidase (GUS) and microarrays (8, 27–29).

In graminaceous plants, the genes encoding MAs biosynthetic enzymes have been isolated from barley (*HvNAS1–7*, *NASHOR1* and *2*, *HvNAAT–A* and *–B*, and *HvDMAS1* (11–13, 30)), maize (*ZmNAS1–3*, *ZmNAAT1* and *ZmDMAS1* (13, 31, 32)) and rice (*OsNAS1–3*, *OsNAAT1* and *OsDMAS1* (13, 32, 33)). The expression levels of these genes are strongly induced in response to Fe deficiency. Histochemical analysis of promoter–GUS rice transformants revealed that these rice genes share highly similar expression patterns, with

significant expression in all cells in Fe-deficient roots (8, 13, 32–34). Fe(III)–MAs uptake transporter genes include members of the *YSL* family, which were first identified in maize (*YS1*) and subsequently isolated from several plants, such as barley (*HvYS1*, rice (*OsYSL1–18*) and *Arabidopsis* (*AtYSL1–8*) (7, 35, 36). The YSL family is involved in the transport of various metal–MAs and metal–NA complexes. For example, YS1 transports various DMA-bound metals including Fe(III), Zn(II), Cu(II), and Ni(II), and also transports NA-chelated Ni(II), Fe(II), and Fe(III) complexes (37). OsYSL15 and OsYSL18 transport Fe(III)–DMA (8, 38), while OsYSL2 transports Fe(II)–NA and Mn(II)–NA (36). OsYSL16 transports Fe(III)–DMA and Cu(II)–NA (29, 39). The expression of *YS1*, *OsYSL2*, *OsYSL15*, and *OsYSL16* are increased in both roots and shoots under conditions of Fe deficiency, whereas the expression of *OsYSL18* is not altered by Fe status. YSL family transporters play important roles in internal metal homeostasis by transporting metal–MAs and metal–NA complexes.

Recently, we identified transporter of MAs (TOM1) as an efflux transporter of DMA in rice, barley, and maize (40, 41). Expression of *TOM1*, *HvTOM1*, and *ZmTOM1* was strongly induced in Fe-deficient roots, while in rice and barley, *TOM1* and *HvTOM1* showed a diurnal pattern in their expression. In transgenic rice with overexpressed or repressed expression of *TOM1*, the level of *TOM1* expression correlates highly with the level of phytosiderophore secretion from the roots. Moreover, overexpression of *TOM1* and *HvTOM1* resulted in increased tolerance to Fe deficiency. These results suggest that *TOM1* is the main transporter for MAs secretion under Fe deficiency. *TOM1*, *HvTOM1*, and *ZmTOM1* are members of the major facilitator superfamily (MFS), which is widely distributed among plants (42). The efflux transporter of NA (ENA1) in rice also belongs to this family (40). ZINC-INDUCED FACILITATOR1 (ZIF1), the ortholog of TOM1 in *Arabidopsis*, was reported to be an efflux transporter of NA localized in the vacuolar membrane and hypothesized to transport NA from the cytoplasm into vacuoles (43, 44). Rice contains five homologs of *TOM1*; two are located in tandem with *TOM1* on chromosome 11 (Os11g0135000; *TOM2* and Os11g0135900; *TOM3*) and three others are located in tandem on chromosome 12 (*Os12g0132500*, *Os12g0132800*, and *Os12g0133100*), similar to *TOM* genes on chromosome 11. However, their functions have not yet been identified. In the present study, we analyzed the function of *TOM2* and *TOM3* in rice to advance our understanding of the role of MAs and their efflux transporters in graminaceous plants. We found that TOM2 has the ability to transport phytosiderophores to the cell exterior and is necessary for normal plant growth.

EXPERIMENTAL PROCEDURES

Gene Cloning—The *TOM2* gene was amplified from a rice (*Oryza sativa* L. cv. Nipponbare) cDNA library (45) template using the primers 5′-CACCA TGGCT GAGCC GCCGG CGAC-3′ and 5′-CTATT TGTAT TGTTG AGGAA-3′. The amplified DNA fragment was subsequently cloned into the pENTR™/D-TOPO® vector (Invitrogen, Carlsbad, CA, USA) to construct the pTOM2 plasmid.

Construction of Plant Expression Vectors and Transgenic Plants—To construct the β-glucuronidase (GUS) reporter fusion genes, 1.5-kb fragments of the 5′ upstream regions of *TOM2* (*Os11g0135000*, AK121911) and *TOM3* (*Os11g0135900*, AK064297) were amplified from rice genomic DNA extracted from rice leaves (cv. Nipponbare) using the primer pairs 5′-CTCGA GCGGT GTATT TTACT CATGA ACAAA-3′ and 5′-TCTAG ACAAC GGCGA CGCTC TCAAT GGAGT-3′, and 5′-CTCGA GTGCT ACTGA TGCTC AACCA GGGCT CTGTT T-3′ and 5′-TCTAG AAGGT CGCCC ATCAA TTCAC CAATC TCGCT C-3′, respectively, and ligated into the pCR4 Blunt-TOPO vector (Invitrogen). The gene fragments were then excised and subcloned into the

pIG121Hm vector (46) upstream of the GUS open reading frame (ORF) to form the *TOM2* promoter–GUS and *TOM3* promoter–GUS constructs. To confirm subcellular localization of *TOM2* in rice plants, an attL/attR substrate recombination reaction between pTOM2 and pH7FWG2 (47) generated the CaMV 35S promoter–*TOM2–enhanced green fluorescent protein* (*eGFP*) cassette. The 3′-noncoding regions from *TOM2* (170 bp) and *TOM3* (297 bp) were amplified from a rice (cv. Nipponbare) cDNA library template (45) using the primer pairs 5′-CACCA TTCAG ATACT GTCAG CT-3′ and 5′-ATGTC ATAGC TTTTG CAAGA-3′, and 5′-CACCT GTTGG CAATT TCATG AGCCC TGCA-3′ and 5′-CTTAC AGAGT TTTAC TAGTT ACAAT GTACA T-3′, respectively, and cloned into the pENTR™/D-TOPO® vector (Invitrogen). The resulting intermediate entry vectors were recombined with the pIG121–RNAi–DEST binary vector (48) using LR Clonase (Invitrogen) according to the manufacturer's instructions to construct the RNAi cassettes *TOM2RNAi* and *TOM3RNAi*. *Agrobacterium tumefaciens* strain C58 carrying these constructs was then used to transform rice (cv. Tsukinohikari) (46).

GUS Activity Assay—GUS activity in the roots and shoots of transgenic plants was determined using a histochemical assay (34). GUS activity in reproductive organs and germinating seeds was also determined histochemically according to previously described methods (27).

Plant Growth Conditions and Elemental Analysis—Rice plants were grown hydroponically. Seeds were surface-sterilized with a 2.5% sodium hypochlorite solution and then germinated for 1 week. After germination, the seedlings were transferred to a 20-L plastic container containing a nutrient solution of the following composition: 0.7 mM K_2SO_4, 0.1 mM KCl, 0.1 mM KH_2PO_4, 2.0 mM $Ca(NO_3)_2$, 0.5 mM $MgSO_4$, 10 μM H_3BO_3, 0.5 μM $MnSO_4$, 0.2 μM $CuSO_4$, 0.5 μM $ZnSO_4$, 0.05 μM Na_2MoO_4, and 0.1 mM Fe(III)–EDTA. The pH of the nutrient solution was adjusted daily to 5.5 with 1 M HCl. Fe deficiency was initiated 4 weeks after germination by transferring the plants to an Fe(III)–EDTA-free culture medium. For chlorophyll analysis, plants were grown hydroponically as described above. At day 12 after transition to the Fe-deficient medium, the youngest and oldest leaves at that time were analyzed for chlorophyll content using a SPAD-5 chlorophyll meter (Konica Minolta, Tokyo, Japan). Plant length and weight were measured 2 weeks after transition to the Fe-deficient medium. Three to five plants for each line were used for each analysis, and the same experiments were replicated three times, and the reproducibility of the experiments was confirmed. The concentrations of Fe, Zn, Cu, and Mn were determined using inductively coupled plasma–mass spectroscopy (ICP-MS) (15). Experiments were all performed in triplicate.

Quantitative Real-Time Polymerase Chain Reaction (*qRT-PCR*)—Total RNA was extracted from the shoots and roots of three plants per each line using the RNeasy Plant Kit (Qiagen, Hilden, Germany), following the manufacturer's instructions, and was treated with RNase-free DNase I (TaKaRa, Otsu, Japan) to remove contaminating genomic DNA. First-strand cDNA was synthesized using ReverTra Ace® reverse transcriptase (Toyobo, Tokyo, Japan) by priming with oligo-$d(T)_{17}$. A fragment was amplified by PCR in a StepOnePlus™ Real-Time PCR system (Applied Biosystems, Foster City, CA, USA) using SYBR Green I and ExTaq™ RealTime-PCR Version (TaKaRa). The primers used for qPCR of *TOM2* and *TOM3* were 5'-ACCTT CTACC CTGTC TTTGT-3' and 5'-CTCCA CTCCT GTTTC AAGGC-3', and 5'-CTGAT GCAAA TAGAT CTCAA-3' and 5'-CTTGC AGTCC AAACT ACCAT-3', respectively. The primers used for qRT-PCR of rice Fe regulated transporter 1 (*OsIRT1*) and rice Fe-related transcription factor 2 (*OsIRO2*) were as described previously (49). The primers used for qRT-PCR of *OsFer*, which recognized both *OsFer1* and *OsFer2*, were *OsFer* forward: 5'-

GTGAA GGGCA GTAGT AGGTT TCG-3', and *OsFer* reverse: 5'-CGCGC GACAT ACACA TGATT CTG-3'. The primers used for the internal control for real-time PCR were *OsActin1* forward: 5'-ACACC GGTGT CATGG TCGG-3', and *OsActin1* reverse: 5'-ACACG GAGCT CGTTG TAGAA-3'. The sizes of the amplified fragments were confirmed by agarose gel electrophoresis.

Construction of Oocyte Expression Vectors and Efflux Experiments—The *TOM2* ORF of pTOM2 was excised from pTOM2 with *Eco*I and *Xho*I, and cloned into a previously constructed plasmid (50). Then capped complementary RNA (cRNA) derived from these plasmids was injected into *Xenopus laevis* oocytes (50). Assays of efflux activity using *X. laevis* oocytes were performed according to a previously described method (40).

Construction of the GFP Fusion Gene for the Transient Expression and Observation of TOM2–synthetic GFP (*sGFP*) *Localization*—An attL/attR substrate recombination reaction between pTOM2 and pDEST35S–sGFP (51) generated an expression vector containing the *Cauliflower mosaic virus* (CaMV) 35S promoter–TOM2–sGFP gene fusion sequence (*35S::TOM2-GFP*). Onion epidermal cells were transformed with *35S::TOM2-GFP* using the Biolistic® PDS-1000/He Particle Delivery System (Bio-Rad Laboratories, Inc., Tokyo, Japan), and sGFP fluorescence was observed (31).

RESULTS

Recently, we isolated *TOM1* (*Os11g0134900*) as an efflux transporter of DMA in rice (40). To characterize the TOM family in rice, we carried out a homology search of TOM1 using a rice genome database (RAP-DB, http://rapdb.dna.affrc.go.jp/) and found five homologous genes of *TOM1*: *TOM2* (*Os11g0135000*), *TOM3* (*Os11g0135900*), *Os12g0132500*, *Os12g0132800*, and *Os12g0133100* (Fig. 1*A*). *TOM1*, *TOM2*, and *TOM3* are located on chromosome 11 in tandem (Fig. 1*B*), while similarly, *Os12g0132500*, *Os12g0132800*, and *Os12g0133100* are located on chromosome 12 in tandem. We compared their genomic sequences and found that the *TOM1*, *TOM2*, and *TOM3* genomic sequences are quite similar to those of *Os12g0132500*, *Os12g0132800*, and *Os12g0133100*, respectively (Fig. 1*C*). The coding sequence of each gene predicted by the genomic sequence was also quite similar. We attempted to clone *Os12g0132500*, *Os12g0132800*, and *Os12g0133100*, but were unsuccessful in cloning their cDNA. Therefore, we focused on analyzing the functions of TOM2 and TOM3 in the present study.

Promoter–GUS Analysis of TOM2 and TOM3—To assess the tissue-specific localization of TOM2 and TOM3, we generated transgenic plants in which the GUS gene *uidA* was driven by the *TOM2* or *TOM3* promoter (Fig. 2). Under Fe-sufficient conditions, *TOM2* and *TOM3* expression was not observed in roots (Fig. 2, *A*, *C*, and *E–G*). *TOM2* expression was induced in roots by Fe deficiency (Fig. 2, *B* and *H–K*), and observed in areas near where the lateral roots emerged (Fig. 2*B*). In cross-section, *TOM2* expression was observed in the cortex and central cylinder, both of which are involved in metal translocation, but not in the exodermis, which is involved in metal uptake from the soil, or in the endodermis (Fig. 2, *H–J*). In vertical section, *TOM2* expression occurred in root radicles, where cell division is active (Fig. 2*K*). Under Fe-deficient conditions, *TOM3* expression was only occasionally detected near the root tips (Fig. 2*D*).

TOM2 expression was also observed in the basal part of the shoots, which is suggested to be important for Fe transfer from xylem to phloem for translocation to the youngest leaf (52). Strong expression was detected near the junction between roots and shoots (Fig. 2, *L* and *M*). The vertical section (Fig. 2*N*) and cross-section (Fig. 2*O*) showed that *TOM2* was expressed in the vascular bundle and root radicles of the basal part of the shoots. In the cross-section of leaf sheaths 5 cm above the basal part of the shoots, *TOM2* expression was observed in large vascular bundles, the outer layer, and veins between large vascular bundles

(Fig. 2*P*). In leaf blades, *TOM2* expression was observed in phloem cells in the large vascular bundles (Fig. 2*Q*). The expression patterns of *TOM2* in the shoots were not altered by Fe status. The expression of *TOM3* was not observed in shoots (data not shown).

TOM2 and *TOM3* expression was also observed in developing and germinating seeds (Fig. 2, *R*, *S*). During seed development, nutrients are transported from leaves through vascular bundles to the embryo and endosperm (53). During germination, these nutrients, accumulated in the endosperm, are transported through epithelium to the embryo (54). In developing seeds, *TOM2* expression was observed in the dorsal vascular bundles, epithelium, and scutellum of the embryo, while *TOM3* expression was observed in the anther and aleurone layer (Fig. 2*R*). In germinating seeds, *TOM2* expression was detected in the epithelium, scutellum, and dorsal vascular bundles, while *TOM3* expression was observed in the aleurone layer (Fig. 2*S*).

Functions of TOM2 and TOM3 in Rice—To examine the function of *TOM2* and *TOM3* in rice plants, transgenic plants in which their expression was repressed using RNA interference (RNAi plants) were generated. qRT-PCR of the RNAi plant roots confirmed that the expression of *TOM2* and *TOM3* was repressed in *TOM2* RNAi and *TOM3* RNAi plants, respectively (Fig. 3, *D* and *E*). In normal soil culture, *TOM2* RNAi plants showed growth defects compared to non-transformants (NTs), while *TOM3* RNAi plants showed no significant differences in vegetative growth (Fig. 3, *A–C*, *F–H*). Tiller number (Fig. 3*A*) and seed fertilities of *TOM2* RNAi plants decreased compared to *TOM3* RNAi and NT plants (Fig. 3, *B* and *C*). Dry weight of the shoots at harvest and yields of *TOM2* RNAi plants were dramatically lower than those of *TOM3* RNAi and NT plants, while shoot length did not significantly differ (Fig. 3 *F-H*). Metal concentrations in the seeds of *TOM2* RNAi, *TOM3* RNAi, and NT rice were measured (Fig. 3*I*). Mn concentrations were higher in *TOM2* RNAi seeds compared to NT and *TOM3* RNAi seeds. Fe, Zn, and Cu concentrations did not significantly differ among *TOM2* RNAi, *TOM3* RNAi, and NT plants.

Next, plants were grown in Fe-deficient hydroponic culture medium to confirm the phenotype of *TOM2* RNAi (Fig. 4, *A–D*). In agreement with the phenotype seen under soil culture, both the shoot and root weights of *TOM2* RNAi were significantly lower than in NTs (Fig. 4, *B* and *D*), although the shoot and root lengths did not significantly differ (Fig. 4, *A* and *C*). In the shoots, Fe requirement is particularly high in newly developing leaves where various Fe-containing proteins, used for various metabolic processes such as photosynthesis, are newly biosynthesized. As a consequence, symptoms of Fe deficiency, namely chlorosis (a decrease in chlorophyll contents), first appear in the youngest leaves. In addition, Fe absorbed from barley roots is transmitted to the youngest leaf and the other leaves mainly via phloem and xylem, respectively (52). Therefore, the chlorophyll contents (in SPAD units) and metal concentration of the oldest leaves and the youngest leaves at the sampling time were measured (Figs. 4 and 5). The SPAD value of the oldest leaves of *TOM2* RNAi plants were lower than in NT plants (Fig. 4*E*), while the SPAD values at the sampling time of the youngest leaves of *TOM2* RNAi plants were slightly lower than in the NTs (Fig. 4*F*). Fe concentrations in the youngest leaves and roots were similar between *TOM2* RNAi plants and NT, while Fe concentrations in the 5th leaves from the youngest leaves and leaf sheath of *TOM2* RNAi lines tended to be higher than in the NTs (Fig. 5). Zn and Cu concentrations in the youngest leaves, leaf sheath, and roots of *TOM2* RNAi lines were higher than in NTs. Moreover, Mn concentrations were significantly higher in the youngest leaves, 5th youngest leaves, and leaf sheaths of *TOM2*RNAi lines compared to NTs.

We further analyzed the change in the expression of genes involved in Fe homeostasis (Fig. 6). The expression levels of *TOM1* and *OsIRO2*, encoding an Fe deficiency-induced

transcription factor regulating Fe homeostasis (55), were slightly higher in lines #2 and #4 of *TOM2* RNAi rice compared to NT plants. In contrast, the expression levels of *TOM3* and *OsIRT1*, encoding a ferrous Fe transporter (56), and *OsYSL2* did not significantly differ between *TOM2* RNAi rice and the NTs. The expression level of *OsFer1* and *OsFer2*, encoding Fe storage proteins ferritins (57) (quantified collectively as *OsFer*), in *TOM2* RNAi rice decreased compared to the NTs in Fe-sufficient roots, while their expression was similar between *TOM2* RNAi rice and NT plants in Fe-deficient roots.

DMA Efflux Activity of TOM2—To examine the DMA transport activity of TOM2, ^{14}C-labeled DMA was synthesized from *S*-adenosyl-^{14}C-L-methionine as previously described (40). We injected capped *TOM2* complementary RNA (cRNA), *TOM1* cRNA (positive control), or water (negative control) into *X. laevis* oocytes and incubated them for 2 days. Then the oocytes were loaded with ^{14}C-labeled DMA and monitored for the release of ^{14}C into the medium (Fig. 7, *A*). Oocytes expressing *TOM2* exhibited a higher rate of DMA efflux than control oocytes (Fig. 7, *A*). TOM2 efflux activity was similar to that of TOM1.

Subcellular localization of the TOM2 protein was investigated by fusing the coding sequence of *TOM2* with GFP. In onion epidermal cells transiently expressing the TOM2–GFP fusion protein, fluorescence was localized to the cell membrane (Fig. 7, *B–D*). In addition, cell membrane localization of the TOM2–GFP fusion protein was confirmed in rice roots stably expressing *TOM2–GFP* (Fig. 7, *E–G*), collectively indicating that *TOM2* encodes a transporter of DMA efflux to the cell exterior.

DISCUSSION

The TOM Gene Family May Be Duplicated in the Rice Genome—The rice genome contains five genes homologous to *TOM1* (Fig. 1*A*). Of these, *TOM1*, *TOM2*, and *TOM3* are tandemly located on chromosome 11, while the three other genes (*Os12g0132500*, *Os12g0132800*, and *Os12g0133000*) are located on chromosome 12, also in tandem (Fig. 1*B*). The gene structure on chromosome 12 is quite similar to *TOM1–3* on chromosome 11. Genomic sequences of the predicted coding regions of *TOM1* and *Os12g0132500* share 98% identity (Fig. 1*C*), while *TOM2* and *Os12g0132800*, and *TOM3* and *Os12g0133000*, show 94% and 97% identity, respectively. We could not find a cDNA clone with the predicted coding sequence of *Os12g0132500*. Therefore, whether *Os12g0132500* is transcribed in rice is uncertain. *TOM2* has several rice Tos17 insertion mutants (http://tos.nias.affrc.go.jp/). We confirmed that Tos17 was definitely inserted into the *TOM2* genomic region, but the expression level of *TOM2* in these mutants, as detected by Northern blot analysis, was not altered compared to the wild type. In addition, *TOM2* Tos17 mutants showed no phenotypic changes as seen in *TOM2* RNAi plants in this study. We could not distinguish the expression between *TOM2* and *Os12g0132800* in *TOM2* Tos17 mutants. *Os12g0132800* expression may complement *TOM2*, and *Os12g0132500*, *Os12g0132800*, and *Os12g0133000* on chromosome 12 may be duplicates of the *TOM* family on chromosome 11. These observations suggest that DMA secretion and transport by the TOM family are important for plant nutrition. The function of the TOM family may be conserved by duplication of the genomic fragment in rice.

TOM2 is Involved in the Internal Transport of Metals by DMA Efflux Transport—MAs are able to chelate Fe and other metals, such as Zn, Cu, and Mn (21, 22). MAs are abundant in rice roots and shoots, and the amount of DMA in the xylem sup increases under Fe deficiency, suggesting that MAs play important roles in internal metal transport (23–25). Moreover, chemical speciation of Fe-binding ligands revealed DMA as a dominant chelator in rice phloem sap (26). These results indicate that MAs play important roles both in Fe acquisition from the soil and in internal metal transport inside the plant body. In the present study, promoter-*GUS* analysis showed that *TOM2* is expressed in the vascular tissues in roots, shoots,

and seeds (Fig. 2). *TOM2* expression was very high in the vascular tissues of the basal part of the shoots, which connects the roots and shoots (Fig. 2*L*-*O*). Using a positron-emitting tracer imaging system, Fe was shown to first accumulate at the basal part of the shoots after absorption from the roots and is then distributed throughout the plant body (52). Thus, TOM2 and DMA might be involved in Fe distribution mediated in this part of the plant. We clarified that TOM2 has efflux activity using ^{14}C-DMA in *X. laevis* oocytes (Fig. 7*A*). In onion epidermal cells and rice roots, TOM2 localized to the cell membrane (Fig. 7, *B*–*G*). These results demonstrate that TOM2 is an efflux transporter of DMA from the cytosol to the cell exterior. Our results suggest that TOM2 is involved in DMA-mediated metal transport inside the plant body and supports the importance of DMA as a chelating molecule facilitating metal transport in the plant body in addition to its well-known function in Fe uptake from the soil.

TOM2 is Crucial for Normal Plant Growth—We observed growth defects in *TOM2* RNAi rice, but not in *TOM3* RNAi rice (Figs. 3 and 4). In *TOM2* RNAi plants, the concentrations of Fe and other metals, such as Zn, Cu, and Mn, tended to be higher than in the NTs in the youngest leaves, 5th youngest leaves, leaf sheath, roots, and seeds (Figs. 3 and 5). These results suggest that metal translocation was aberrant in *TOM2* RNAi plants. Previously, phenolics efflux zero 1 and 2 (PEZ1 and PEZ2), the efflux transporters of protocatechuic acid, were reported to contribute to the long-distance transport of Fe through the solubilization of precipitated apoplasmic Fe in the root xylem (58, 59), suggesting that some transporters are necessary to mobilize metals accumulated in the apoplasm to transport them to sinks in plants. Members of the YSL family in rice are also involved in the internal transport of metals. OsYSL15, which imports Fe(III)–DMA, is strongly expressed in Fe-deficient roots, which suggests that OsYSL15 functions in the absorption of Fe(III)–DMA from the soil (8). In addition, the expression of *OsYSL15* was observed in seeds, and its repression by RNAi led to defects in seed germination, suggesting that OsYSL15 is also involved in the internal transport of Fe. OsYSL2, which imports Fe(II)–NA and Mn(II)–NA, is strongly expressed in Fe-deficient leaves (36). Enhancement of *OsYSL2* expression driven by a sucrose transporter promoter increased the Fe concentration in polished seeds up to 4.4-fold compared to the NTs (60). These results suggest that OsYSL2 is important for phloem transport of metals into seeds. In addition, OsYSL16 and OsYSL18, Fe(III)–DMA transporters, are specifically expressed in the xylem or phloem and reproductive organs (29, 38, 61). These results suggest that the expression of specialized transporters in restricted areas is necessary to maintain metal homeostasis throughout the plant body. Promoter–*GUS* analysis in the present study indicated that *TOM2* is expressed in the vascular tissues of shoots and seeds under both Fe-sufficient and Fe-deficient conditions (Figs. 2, *L*-*S*). In addition, under Fe-deficient conditions, *TOM2* expression was high in the vascular tissues of roots (Fig. 2*B*, *H*-*K*). These expression patterns are consistent with an analysis of transcriptomes by laser microdissection microarray, in which *TOM2* was expressed mainly in the vascular bundles and induced by Fe deficiency in the cortex (62). TOM2 expression was very high in the root primordium during the vegetative stage (Fig. 2*B*, *K*) and in the embryo during the reproductive stage and germination (Fig. 2*R*). These expression patterns suggest that TOM2 is involved in the mobilization of metals through the secretion of DMA into the vascular bundles for phloem and/or xylem metal loading to supply sufficient metals for plant differentiation and growth. In *TOM2* RNAi rice, the expression level of *OsFer* (summation of *OsFer1* and *OsFer2*) was lower than in the NTs, and the expression of other Fe homeostasis-related genes, such as *TOM1* and *OsIRO2*, tended to be induced (Fig. 6). *OsFer1* and *OsFer2* encode the Fe storage protein ferritin, which releases Fe under Fe deficiency (57). The expression levels of *OsFer1* and *OsFer2* are downregulated under

Fe deficiency and upregulated under Fe excess conditions (57). Decreases in *OsFer* expression and the slight induction of *TOM1* and *OsIRO2* in *TOM2* RNAi rice suggest that *TOM2* RNAi plants are physiologically deficient in Fe compared to NT plants. TOM2 may play a crucial role in metal mobilization and utilization in the apoplasm through DMA secretion to solubilize metal nutrients to facilitate their transport to sinks in the plant body.

In conclusion, we showed that the TOM family has important roles both in the acquisition of Fe from the soil and in metal translocation in graminaceous plants through the efflux transport of DMA. *TOM1* expression increases dramatically under Fe-deficient conditions and may be involved mainly in the secretion of phytosiderophores into the soil from root cells (40). In contrast, TOM2 may function primarily in the translocation of metals inside the plant body under normal growth conditions. The function of TOM3 has not yet been determined, but is thought to also have a specific role in the transport of phytosiderophores because of sequence similarity to TOM1 and TOM2. The TOM family has important roles in the maintenance of metal homeostasis through the secretion of DMA into the soil and also by translocation of metals to sink areas in plants. In addition, analogy between MAs and NA suggests that the TOM family is also involved in NA-mediated metal translocation in all higher plants. Recent advances have shown that specialized plant membrane transporters can be used to enhance the yields of staple crops and increase the nutrient content and resistance to key stresses, such as Fe deficiency, which could expand the amount of available arable land (63). Characterization of the TOM family is a significant step in advancing these efforts.

Acknowledgments- We thank Ms. A. Sato for technical support with the oocyte experiments.

Conflict of interest- The authors declare no conflicts of interest.

Author contributions- TN designed, performed, analyzed experiments and wrote the paper. SN provided technical assistance in the experiments shown in Figure 3. TK and HN provided assistance writing the paper. YS and NU provided technical assistance performing experiments shown in Figure 7. NKN conceived and coordinated the study and wrote the paper with TN. All authors reviewed the results and approved the final version of the manuscript.

REFERENCES

1. Römheld, V., and Marschner, H. (1986) *Plant Physiol.* **80**, 175–180
2. Eide, D., Broderuis, M., Fett, J., and Guerinot, M. L. (1996) *Proc. Natl. Acad. Sci. U. S. A.* **93**, 5624–5628
3. Robinson, N. J., Procter, C. M., Connolly, E. L., and Guerinot, M. L. (1999) *Nature* **397**, 694–697
4. Vert, G., Grotz, N., Dedaldechamp, F., Gaymard, F., Guerinot, M. L., Briat, J. F., and Curie, C. (2002) *Plant Cell* **14**, 1223–1233
5. Takagi, S. (1976) Naturally occurring iron-chelating compounds in oat-and rice-root washings : I. Activity Measurement and Preliminary Characterization. *Soil Sci Plant Nutr* **45**, 993-1002
6. Takemoto, T., Nomoto, K., Fushiys, S., Ouchi, R., Kusano, G., Hikino, H., Takagi, S., Matsuura, Y., and Kakudo, M. (1978) Structure of Mugineic Acid, a New Amino Acid Possessing an Iron-Chelating Activity from Roots Washings of Water-Cultured Hordeum vulgare L. *Proceedings of the Japan Academy, Series B* **54**, 469-4

7. Curie, C., Panaviene, Z., Loulergue, C., Dellaporta, S. L., Briat, J. F., and Walker, E. L. (2001) Maize yellow stripe1 encodes a membrane protein directly involved in Fe(III) uptake. *Nature* **409**, 346-349
8. Inoue, H., Kobayashi, T., Nozoye, T., Takahashi, M., Kakei, Y., Suzuki, K., Nakazono, M., Nakanishi, H., Mori, S., and Nishizawa, N. K. (2009) Rice OsYSL15 is an iron-regulated iron(III)-deoxymugineic acid transporter expressed in the roots and is essential for iron uptake in early growth of the seedlings. *J Biol Chem* **284**, 3470-3479
9. Mori, S., and Nishizawa, N. (1987) Methionine as a dominant precursor of phytosiderophores in graminaceae plants. *Plant and Cell Physiol* **28**, 1081-1092
10. Shojima, S., Nishizawa, N. K., Fushiya, S., Nozoe, S., Irifune, T., and Mori, S. (1990) Biosynthesis of Phytosiderophores : In Vitro Biosynthesis of 2'-Deoxymugineic Acid from l-Methionine and Nicotianamine. *Plant Physiol* **93**, 1497-1503
11. Higuchi, K., Suzuki, K., Nakanishi, H., Yamaguchi, H., Nishizawa, N. K., and Mori, S. (1999) Cloning of nicotianamine synthase genes, novel genes involved in the biosynthesis of phytosiderophores. *Plant Physiol* **119**, 471-480
12. Takahashi, M., Yamaguchi, H., Nakanishi, H., Shioiri, T., Nishizawa, N. K., and Mori, S. (1999) Cloning two genes for nicotianamine aminotransferase, a critical enzyme in iron acquisition (Strategy II) in graminaceous plants. *Plant Physiol* **121**, 947-956
13. Bashir, K., Inoue, H., Nagasaka, S., Takahashi, M., Nakanishi, H., Mori, S., and Nishizawa, N. K. (2006) Cloning and characterization of deoxymugineic acid synthase genes from graminaceous plants. *J Biol Chem* **281**, 32395-32402
14. Takagi, S., Nomoto, K., and Takemoto, T. (1984) Physiological aspect of mugineic acid, a possible phytosiderophore of graminaceous plants. *J Plant Nutr* **7**, 469-477
15. Nozoye T, Nagasaka S, Bashir K, Takahashi M, Kobayashi T, Nakanishi H, Nishizawa NK. (2014) Nicotianamine synthase 2 localizes to the vesicles of iron-deficient rice roots, and its mutation in the YXXφ or LL motif causes the disruption of vesicle formation or movement in rice. *Plant J* **77**, 246-260
16. Stephan, U. W., and Scholz, G. (1993) Nicotianamine: mediator of transport of iron and heavy metals in the phloem? *Physiol Plant* **88**, 522-529
17. Pich, A., and Scholz, G. (1996) Translocation of copper and other micronutrients in tomato plants (*Lycopersicon esculentum* Mill.): nicotianamine-stimulated copper transport in the xylem. *J Exp Bot* **47**, 41-47
18. Higuchi, K., Kanazawa, K., Nishizawa, N. K., and Mori, S. (1996) The role of nicotianamine synthase in response to Fe nutrition status in Gramineae. *Plant and Soil* **178**, 171-177
19. Ling H, Q., Koch, G., Bäumlein, H., and Ganal, M. (1999) Map-based cloning of *chloronerva*-a gene involved in iron uptake of higher plants encoding nicotianamine synthase. *Proc Natl Acad Sci U S A* **96**, 7098-7103
20. Takahashi, M., Terada, Y., Nakai, I., Nakanishi, H., Yoshimura, E., Mori, S., and Nishizawa, N. K. (2003) Role of nicotianamine in the intracellular delivery of metals and plant reproductive development. *Plant Cell* **15**, 1263-1280
21. von Wirén, N., Klair, S., Bansal, S., Briat, J. F., Khodr, H., Shioiri, T., Leigh, R. A. and Hider, R. C. (1999) Nicotianamine chelates noth Fe^{III} and Fe^{II}. Implications for metal transport in plants[1]. *Plant Physiol* **119**, 1107-1114.
22. Murakami, T., Ise, K., Hayakawa, K., Kamei, S. and Takagi, S. (1989) Stabilities of metal complexes of mugineic acids and their specific affinities for iron(III). Chemistry Letters 2137-2140.
23. Mori, S., Nishizawa, N., Hayashi, H., Chino, M., Yoshimura, E. and Ishihara, J. (1991) Why are young rice plaants highly susceptible to Fe-deficiency ? *Plant and Soil* **130**, 143-156

24. Kawai, S., Kamei, S., Matsuda, Y., Ando, R., Kondo, S., Ishizawa, A., and Alam, S. (2001) Concentrations of iron and phytosiderophores in xylem sap of iron-deficient barley plants. *Soil Sci Plant Nutr* **47**, 265-272
25. Kakei, Y., Yamaguchi, I., Kobayashi, T., Takahashi, M., Nakanishi, H., Yamakawa, T., and Nishizawa, N. K. (2009) A highly sensitive, quick and simple quantification method for nicotianamine and 2'-deoxymugineic acid from minimum samples using LC/ESI-TOF-MS achieves functional analysis of these components in plants. *Plant Cell physiol* **50**, 1988-1993
26. Nishiyama, R., Kato, M., Nagata, S., Yanagisawa, S. and Yoneyama, T. (2012) Identification of Zn-nicotianamine and Fe-2'-deoxymugineic acid in the phloem sap from rice plants. *Plant Cell Physiol* **53**, 381-390
27. Nozoye, T., Inoue, H., Takahashi, M., Ishimaru, Y., Nakanishi, H., Mori, S., and Nishizawa, N. K. (2007) The expression of iron homeostasis-related genes during rice germination. *Plant Mol Biol* **64**, 35-47
28. Takahashi, M., Nozoye, T., Kitajima, N., Fukuda, N., Hokura, A., Terada, Y., Nakai, I., Ishimaru, Y., Kobayashi, T., Nakanishi, H., and Nishizawa, N. K. (2009) In vivo analysis of metal distribution and expression of metal transporters in rice seed during germination process by microarray and X-ray fluorescence imaging of Fe, Zn, Mn, and Cu. *Plant and Soil* **325**, 39-5122.
29. Kakei, Y., Ishimaru, Y., Kobayashi, T., Yamakawa, T., Nakanishi, H., and Nishizawa, N. K. (2012) OsYSL16 plays a role in the allocation of iron. *Plant Mol Biol* **79**, 583-594
30. Herbik, A., Koch, G., Mock, H.P., Dushkov, M., Czihal, A., Thielmann, J., Stephan, U.W. and Ba¨ umlein, H. (1999) Isolation, characterization and cDNA cloning of nicotianamine synthase from barley. A key enzyme for iron homeostasis in plants. *Eur. J. Biochem.* **265**, 231–239.
31. Mizuno, D., Higuchi, K., Sakamoto, T., Nakanishi, H., Mori, S. and Nishizawa, N.K. (2003) Three nicotianamine synthase genes isolated from maize are differentially regulated by iron nutritional status. *Plant Physiol.*, **132**, 1989-1997.
32. Inoue, H., Takahashi, M., Kobayashi, T., Suzuki, M., Nakanishi, H., Mori, S., and Nishizawa, N. K. (2008) Identification and localisation of the rice nicotianamine aminotransferase gene OsNAAT1 expression suggests the site of phytosiderophore synthesis in rice. *Plant Mol Biol* **66**, 193-203
33. Higuchi, K., Watanabe, S., Takahashi, M., Kawasaki, S., Nakanishi, H., Nishizawa, N.K. and Mori, S. (2001) Nicotianamine synthase gene expression differs in barley and rice under Fe-deficient conditions. *Plant J.* **25**, 159–167.
34. Inoue, H., Higuchi, K., Takahashi, M., Nakanishi, H., Mori, S., and Nishizawa, N. K. (2003) Three rice nicotianamine synthase genes, OsNAS1, OsNAS2, and OsNAS3 are expressed in cells involved in long-distance transport of iron and differentially regulated by iron. *Plant J* **36**, 366-381
35. Murata, Y., Ma, J.F., Yamaji, N., Ueno, D., Nomoto, K. and Iwashita, T. (2006) A specific transporter for iron(III)–phytosiderophore in barley roots. *The Plant J.*, **46**, 563-572.
36. Koike, S., Inoue, H., Mizuno, D., Takahashi, M., Nakanishi, H., Mori, S., and Nishizawa, N. K. (2004) OsYSL2 is a rice metal-nicotianamine transporter that is regulated by iron and expressed in the phloem. *Plant J* **39**, 415-424
37. Schaaf, G., Ludewig, U., Erenoglu, B.E., Mori, S., Kitahara, T. and von Wirén, N. (2004) ZmYS1 functions as a proton-coupled symporter for phytosiderophore- and nicotianamine-chelated Metals. *J. Biol. Chem.*, **279**, 9091-9096.

38. Aoyama, T., Kobayashi, T., Takahashi, M., Nagasaka, S., Usuda, K., Kakei, Y., Ishimaru, Y., Nakanishi, H., Mori, S., and Nishizawa, N. K. (2009) OsYSL18 is a rice iron(III)-deoxymugineic acid transporter specifically expressed in reproductive organs and phloem of lamina joints. *Plant Mol Biol* **70**, 681-692
39. Zheng, L., Yamaji, N., Yokosho, K., Ma, J.F. (2012) YSL16 is a phloem-localized transporter of the copper-nicotianamine complex that is responsible for copper distribution in rice. *Plant Cell* **24**, 3767-82
40. Nozoye, T., Nagasaka, S., Kobayashi, T., Takahashi, M., Sato, Y., Uozumi, N., Nakanishi, H., and Nishizawa, N. K. (2011) Phytosiderophore efflux transporters are crucial for iron acquisition in graminaceous plants. *J Biol Chem* **286**, 5446-5454
41. Nozoye, T., Nakanishi, H., and Nishizawa, N. K. (2013) Characterizing the Crucial Components of Iron Homeostasis in the Maize Mutants ys1 and ys3. *PLoS One* **8**, e62567
42. Pao, S. S., Paulsen, I. T., and Saier, M. H. (1998) Major facilitator superfamily. *Microbiol Mol Biol Rev* **62**, 1-34
43. Haydon, M. J., Cobbett, C. S. A. (2007) A novel major facilitator superfamily protein at the tonoplast influences zinc tolerance and accumulation in Arabidopsis. *Plant Physiol.* **143**, 1705-19
44. Haydon, M.J., Kawachi, M., Wirtz, M., Hillmer, S., Hell, R., Krämer, U. (2012) Vacuolar nicotianamine has critical and distinct roles under iron deficiency and for zinc sequestration in Arabidopsis. *Plant Cell* **24**, 724–37.
45. Ishimaru Y, Suzuki M, Tsukamoto T, Suzuki K, Nakazono M, Kobayashi T, Wada Y, Watanabe S, Matsuhashi S, Takahashi M, Nakanishi H, Mori S, Nishizawa NK. Rice plants take up iron as an Fe^{3+}-phytosiderophore and as Fe^{2+}. Plant J. 2006 Feb;45(3):335-46.
46. Hiei, Y., Ohta, S., Komari, T., and Kumashiro, T. (1994) Efficient transformation of rice (Oryza sativa L.) mediated by Agrobacterium and sequence analysis of the boundaries of the T-DNA. *Plant J* **6**, 271-282
47. Karimi, M., Inzé, D., and Depicker, A. (2002) GATEWAY (TM) vectors for Agrobacterium-mediated plant transformation. *Trends. In plant Science* **7**, 193-195
48. Ogo, Y., Itai, R. N., Nakanishi, H., Kobayashi, T., Takahashi, M., Mori, S., and Nishizawa, N. K. (2007) The rice bHLH protein OsIRO2 is an essential regulator of the genes involved in Fe uptake under Fe-deficient conditions. *Plant J* **51**, 366-377
49. Kobayashi, T., Itai, R. N., Ogo, Y., Kakei, Y., Nakanishi, H., Takahashi, M., and Nishizawa, N. K. (2009) The rice transcription factor IDEF1 is essential for the early response to iron deficiency, and induces vegetative expression of late embryogenesis abundant genes. *Plant J* **60**, 948-961
50. Kato, Y., Sakaguchi, M., Mori, Y., Saito, K., Nakamura, T., Bakker, E. P., Sato, Y., Goshima, S., and Uozumi, N. (2001) Evidence in support of a four transmembrane-pore-transmembrane topology model for the Arabidopsis thaliana Na+/K+ translocating AtHKT1 protein, a member of the superfamily of K+ transporters. *Proc Natl Acad Sci U S A* **98**, 6488-6493
51. Ishimaru, Y., Suzuki, M., Kobayashi, T., Takahashi, M., Nakanishi, H., Mori, S., and Nishizawa, N. K. (2005) OsZIP4, a novel zinc-regulated zinc transporter in rice. *J Exp Bot* **56**, 3207-3214
52. Tsukamoto, .T, Nakanishi, H., Uchida, H., Watanabe, S., Matsuhashi, S., Mori, S., Nishizawa, N.K. (2009) ^{52}Fe translocation in barley as monitored by a positron-emitting tracer imaging system (PETIS): Evidence for the direct translocation of Fe from roots to young leaves via phloem. *Plant & Cell Physiology* **50**, 48-57.
53. Hoshikawa, K. (1975) Anatomical illustrations on the rice growth. Kaibo zusetsu Ine no seicho, Nobunkyo, Tokyo. Japan

54. Hoshikawa, K. (1984) Development of endosperm tissuewith special reference to the translocation of reserve substances in cereals. 3, Translocation pathways in rice endosperm. *Japn. Jour. Crop Sci.*, **53**, 153-162.
55. Ogo, Y., Itai, R.N., Nakanishi, H., Inoue, H., Kobayashi, T., Suzuki, M., Takahashi, M., Mori, S. and Nishizawa, N.K. (2006) Isolation and characterization of IRO2, a novel iron-regulated bHLH transcription factor in graminaceous plants. *J Exp Bot* **57**, 867-78
56. Bughio, N., Yamaguchi, H., Nishizawa, N.K., Nakanishi, H. and Mori, S. (2002) Cloning an iron-regulated metal transporter from rice. *J Exp Bot* **53**, 1677-82
57. Stein, R. J., Ricachenevsky, F. K. and Fett, J. P. (2009) Differential regulation of the two rice ferritin genes (**OsFER1** and **OsFER2**). *Plant science* **177**, 563-569.
58. Ishimaru, Y., Kakei, Y., Shimo, H., Bashir, K., Sato, Y., Uozumi, N., Nakanishi, H., and Nishizawa, N. K. (2011) A rice phenolic efflux transporter is essential for solubilizing precipitated apoplasmic iron in the plant stele. *J Biol Chem* **286**, 24649-24655
59. Bashir, K., Ishimaru, Y., Shimo, H., Nagasaka, S., Fujimoto, M., Takanashi, H., Tsutsumi, N., An, G., Nakanishi, H. and Nishizawa, N.K. (2011) Rice phenolics efflux transporter 2 (PEZ2) plays an important role in solubilizing apoplasmic iron. *Soil Sci. Plant Nut*., **57**, 803-812
60. Ishimaru, Y., Masuda, H., Bashir, K., Inoue, H., Tsukamoto, T., Takahashi, M., Nakanishi, H., Aoki, N., Hirose, T., Ohsugi, R., Nishizawa, N.K. (2010) Rice metal-nicotianamine transporter, OsYSL2, is required for long distance transport of iron and manganese. *Plant Journal* 62: 379-390.
61. Lee, S., Ryoo, N., Jeon, J.S., Guerinot, M.L., An, G. (2012) Activation of rice Yellow Stripe1-Like 16 (OsYSL16) enhances iron efficiency. *Mol Cells* **33**, 117-126
62. Ogo, Y., Kakei, Y., Itai, R. N., Kobayashi, T., Nakanishi, H., Takahashi, H., Nakazono, M., Nishizawa, N. K. (2013) Spatial transcriptomes of iron-deficient and cadmium-stressed rice. *New Phytol* **201**, 781-794
63. Schroeder, J. I., Delhaize, E., Frommer, W. B., Guerinot, M. L., Harrison, M. J., Herrera-Estrella, L., Horie, T., Kochian, L. V., Munns, R., Nishizawa, N. K., Tsay, Y. F., and Sanders, D. (2013) Using membrane transporters to improve crops for sustainable food production. *Nature* **497**, 60-66

FOOTNOTES

***** This work was supported by a Grant-in-Aid for Scientific Research on Priority Areas from the Ministry of Education, Culture, Sports, Science and Technology, Japan (to N. K. N and N. U.) and by a a Grant-in-Aid for Young Scientists (B) Grant Number 15K18658 from JSPS KAKENHI (to T. N.).

The abbreviations used are DMA, 2'-deoxymugineic acid; GFP, green fluorescent protein; GUS, β-glucoronidase; NA, nicotianamine; NAAT, nicotianamine aminotransferase; NAS, nicotianamine synthase; *TOM1–3*, transporter of mugineic acid 1–3; and *YSL*, yellow stripe-like.

The nucleotide sequence data reported in this paper are deposited in the RAP-DB/DDBJ/GenBank/TIGR nucleotide sequence databases under the accession numbers BR000946.1 (AK069533, Os11g0134900), AK121911 (Os11g0135000), AK064297 (Os11g0135900), Os12g0132500, Os12g0132800, and Os12g0133000.

FIGURE LEGENDS

FIGURE 1. Gene structure of the rice *TOM* family. (A) Phylogenic tree of the rice *TOM* family. (B) Gene loci of the *TOM* family in the rice genomic sequence (RAP-DB; http://rapdb.dna.affrc.go.jp/). Loci with transcript data (cDNA, mRNA, or ESTs) or protein homologs are shown. (C) Alignment map of the genomic sequences between *TOM1* and Os12g0132500, *TOM2* and Os12g0132800, and *TOM3* and Os12g0133100. The genomic region represents the predicted coding sequence for each

gene. The matches in the sequence are shown in yellow.

FIGURE 2. Tissue distribution of *TOM2* and *TOM3* promoter activity (A–K), in rice shoots during the vegetative stage (L-Q) and in rice during seed development (R) and germination (S) as observed by GUS staining. (A, E–G) Tissue distribution of *TOM2* in Fe-sufficient roots. (B, H–K) Tissue distribution of *TOM2* in Fe-deficient roots. (C, D) Tissue distribution of *TOM3* in Fe-sufficient (C) and Fe-deficient (D) roots. (A–D) The roots on the left side of each panel are the regions in which the lateral roots were elongated. The roots on the right side of each panel are the elongation zones. (E–G) Cross-sections of the iron (Fe)-sufficient root elongation zone. (H–J) Cross-sections of the Fe-deficient root elongation zone. (K) Vertical section of the Fe-deficient root. (L-Q) Tissue distribution of *TOM2* in Fe-sufficient root-shoot junctions and shoots. The basal part of the shoot was cut vertically, and the interior (L) and exterior (M) parts were observed. (N) Enlarged image of the interior side of the basal part of the shoots. (O–Q) Cross-sections of the basal part of the shoots (O), leaf sheath (P), and leaf blade (Q). o: outer layer, b: vascular bundle, v: vein between the large vascular bundles. (R) Tissue-distribution of *TOM2* and *TOM3* in developing seeds. Seeds before anthesis, after fertilization, 5, 8, 20, and 30 days after flowering (DAF), and immediately before full maturation. (S) Tissue distribution of *TOM2* and *TOM3* in germinating seeds. Fully mature seeds (0 d) and germinating rice seeds 1–3 days after sowing. Scale bars; 1 mm (A-D, L-N, R-S), 500 μm (K, O), 200 μm (P, Q), 100 μm (E, H), 50 μm (F,G, I, J).

FIGURE 3. Characteristics of *TOM2* and *TOM3* RNAi rice. (A) Non-transformant (NT), *TOM2* RNAi, and *TOM3* RNAi rice at the maturation stage. (B, C) Maturing seeds of *TOM2* RNAi rice (B) and NT rice (C). (D, E) Quantitative RT-PCR analysis of the *TOM2* RNAi lines (#2, #4 and #16) (D) or *TOM3* RNAi lines (#12, #19 and #21) (E) and NT rice using the *TOM2* or *TOM3* 3'-noncoding region, respectively. The values were normalized to the expression of *OsActin1*. Shoot length (F), shoot weight (G), and yield (H) of each plant at harvest. (I) Iron (Fe), zinc (Zn), copper (Cu), and manganese (Mn) concentrations in the seeds of NT (four plants (1–4)), *TOM2* RNAi (two plants (1–2) from line #2 and #16), and *TOM3* RNAi rice (two plants (1–2) from line #12, #19 and #21). Values represent the means of three replicates. Error bars represent the standard deviation. DW: dry weight.

FIGURE 4. Plant phenotype of *TOM2* RNAi rice grown hydroponically under iron (Fe)-deficient conditions. Shoot length (A), shoot weight (B), root length (C), and root weight (D) of *TOM2* RNAi rice and non-transformant (NT) were measured after 2 weeks of the Fe-deficient treatment. SPAD values (chlorophyll content) of the oldest (E) and youngest (F) leaves of *TOM2* RNAi and NT plants under Fe-deficiency stress (12 d). Error bars represent the standard error (n = 9). FW: fresh weight. Asterisks indicate significant differences compare to the values for NT rice (two-sample Student's t-test; *P<0.05; **P<0.01).

FIGURE 5. Iron (Fe), zinc (Zn), copper (Cu), and manganese (Mn) concentrations in the youngest leaves, 5th youngest leaves, leaf sheaths, and roots of non-transformant (NT) and *TOM2* RNAi rice. Values shown are the means of nine replicates. Error bars represent the standard deviation. DW= dry weight. The values in the bars followed by different letters differ significantly from each other according to the Tukey–Kramer HSD test (n = 9, P < 0.05).

FIGURE 6. Quantitative real-time PCR analysis of *TOM1*, *TOM3*, *OsIRO2*, *OsIRT1*, *OsYSL2*, and *OsFer* expression in non-transformant (NT) and *TOM2* RNAi rice. RNA was extracted from the root under Fe-sufficient (+Fe) or Fe-deficient (-Fe) conditions. The values are shown as relative expression

against the expression of *OsActin1*. Error bars represent the standard deviation.

FIGURE 7. Transporter function of TOM2. (A) Efflux activity of TOM2 in *Xenopus laevis* oocytes. TOM1 was used as a positive control. Oocytes expressing *TOM2* or *TOM1* and control oocytes (injected with water) were injected with ^{14}C-DMA, and the efflux of ^{14}C was measured for 2 h. Values are expressed as the percentage of the total radioactivity injected. Data shown represent the mean ± standard deviation (n = 3). (B–G) Subcellular localization of TOM2–GFP fusion in onion epidermal cells (B–D) and in the endodermis of rice roots (E–G). (B, E) Differential interference contrast (DIC) image. (C, F) Fluorescent image. (D, G) Overlay.

Figure 1

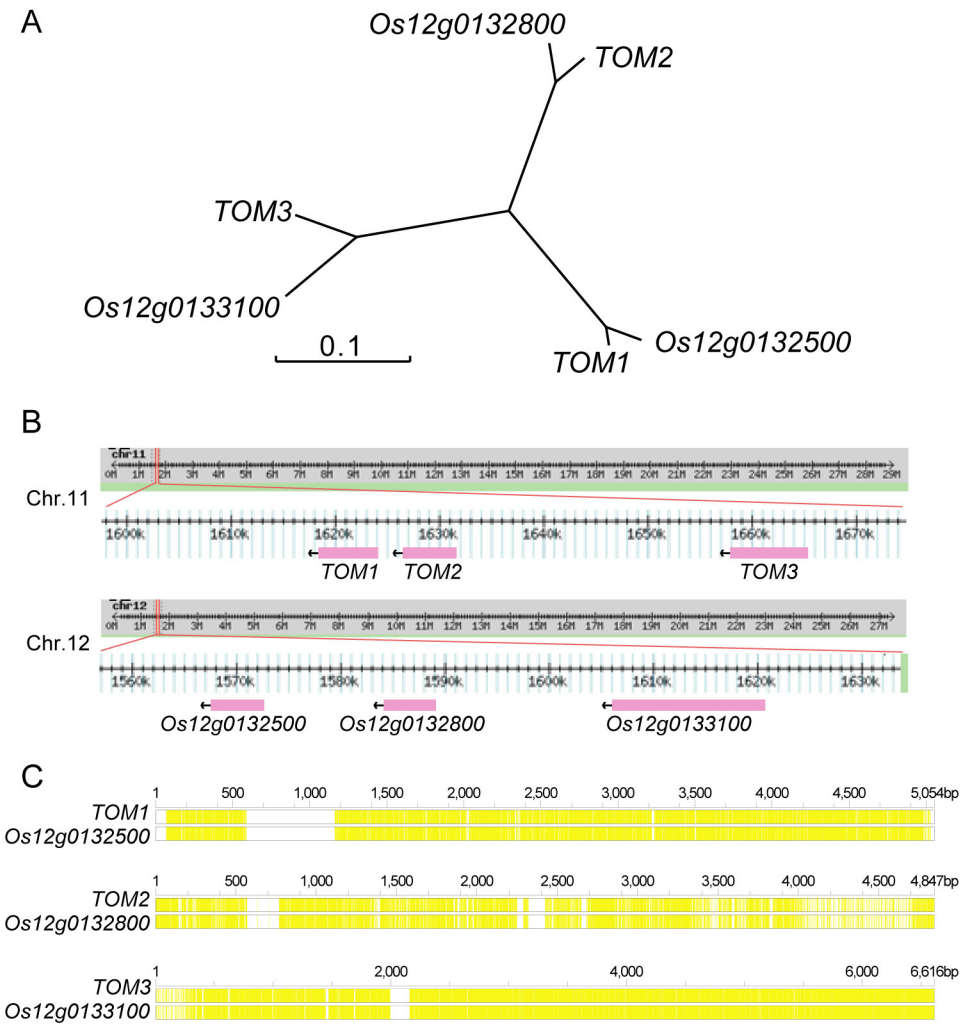

Figure 2

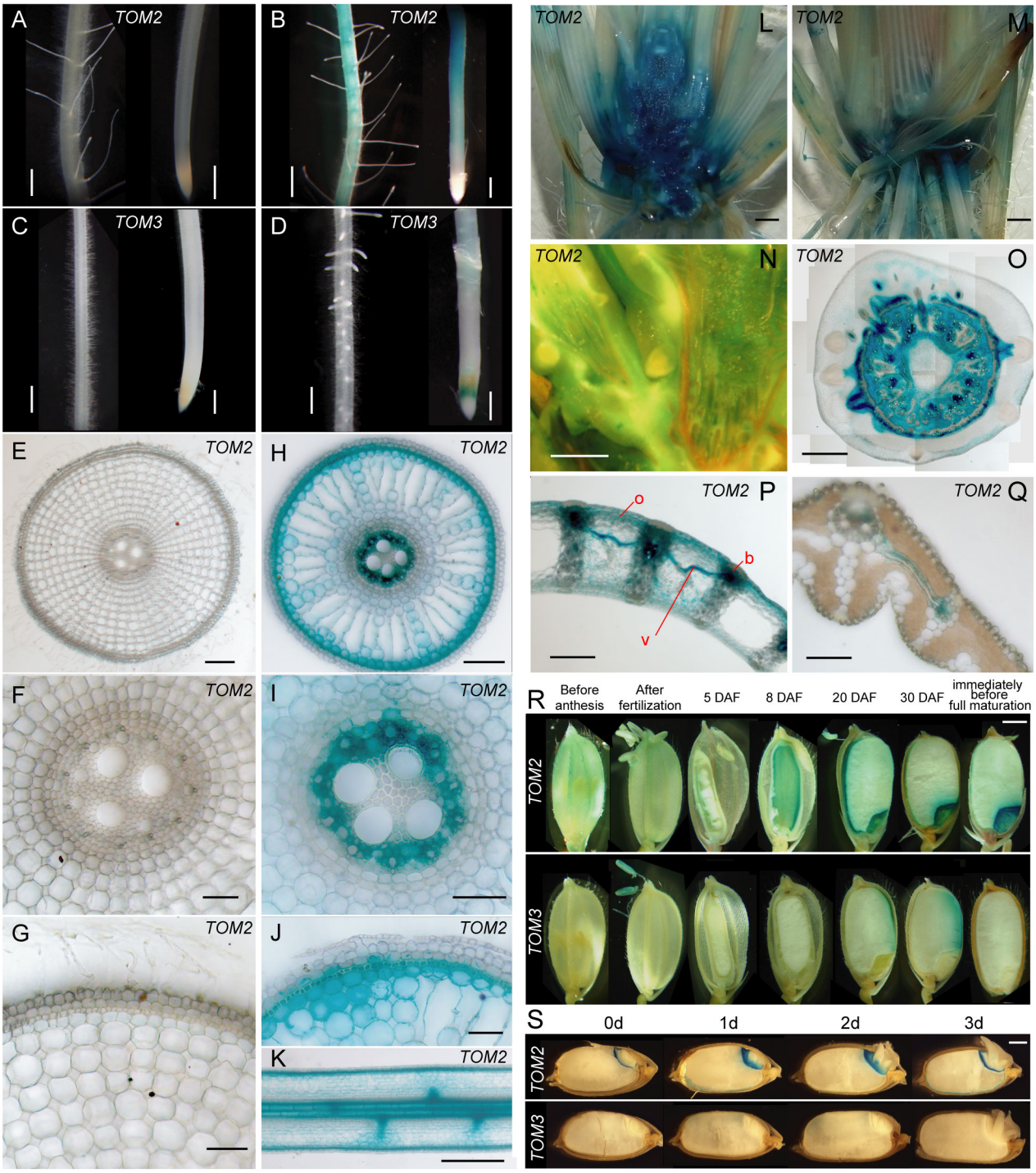

Figure 3

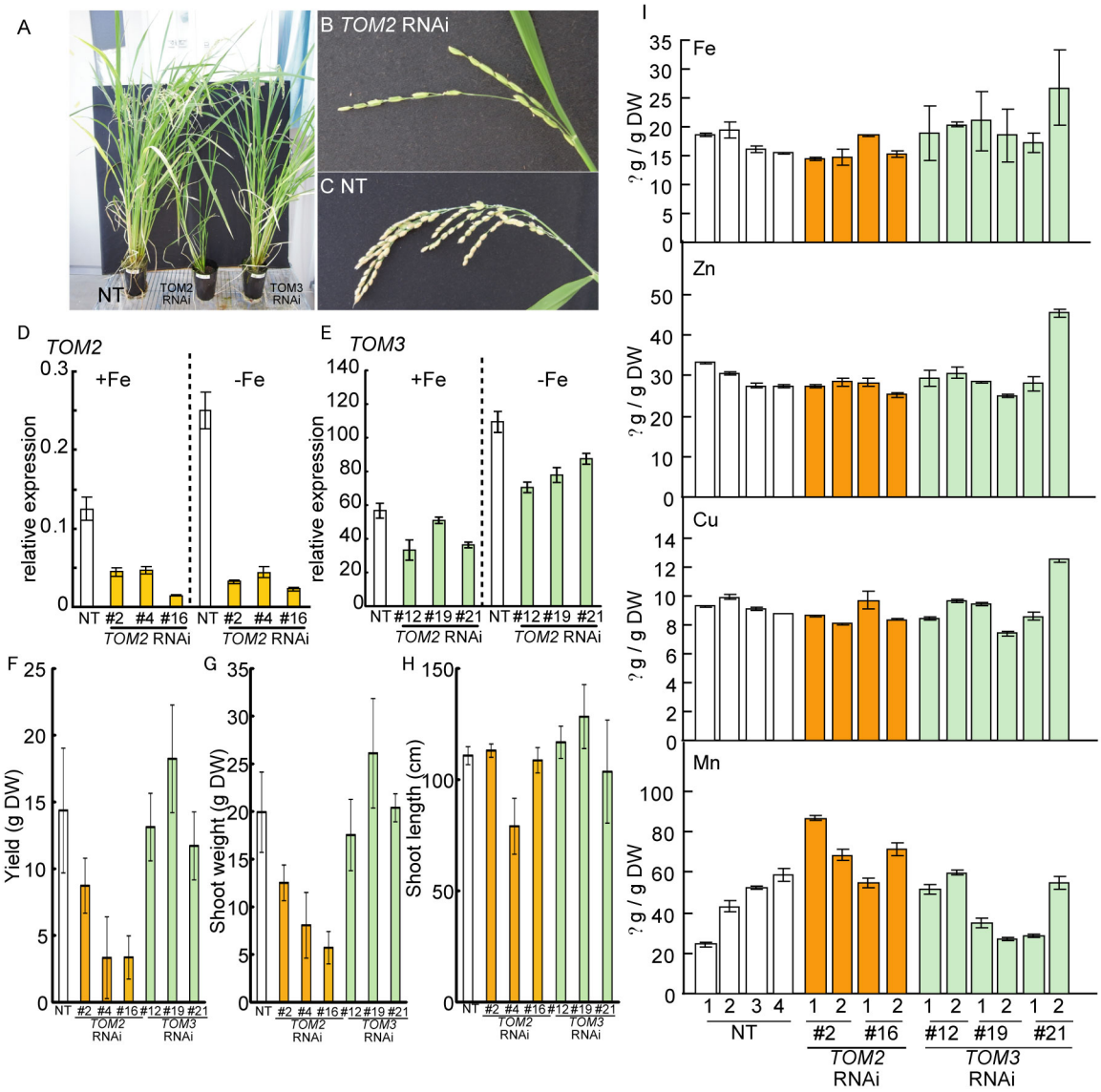

Figure 4

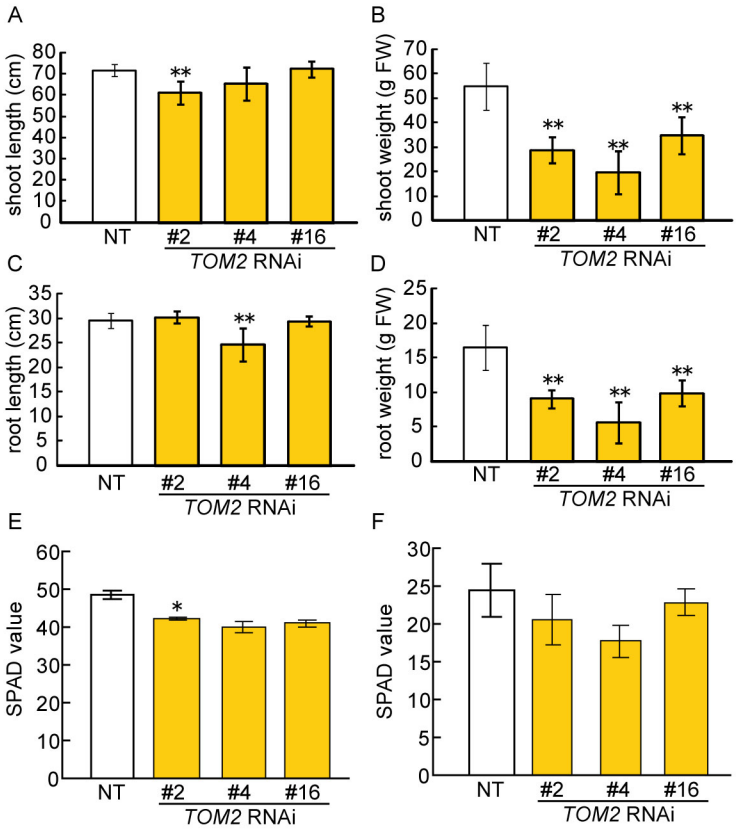

Figure 5

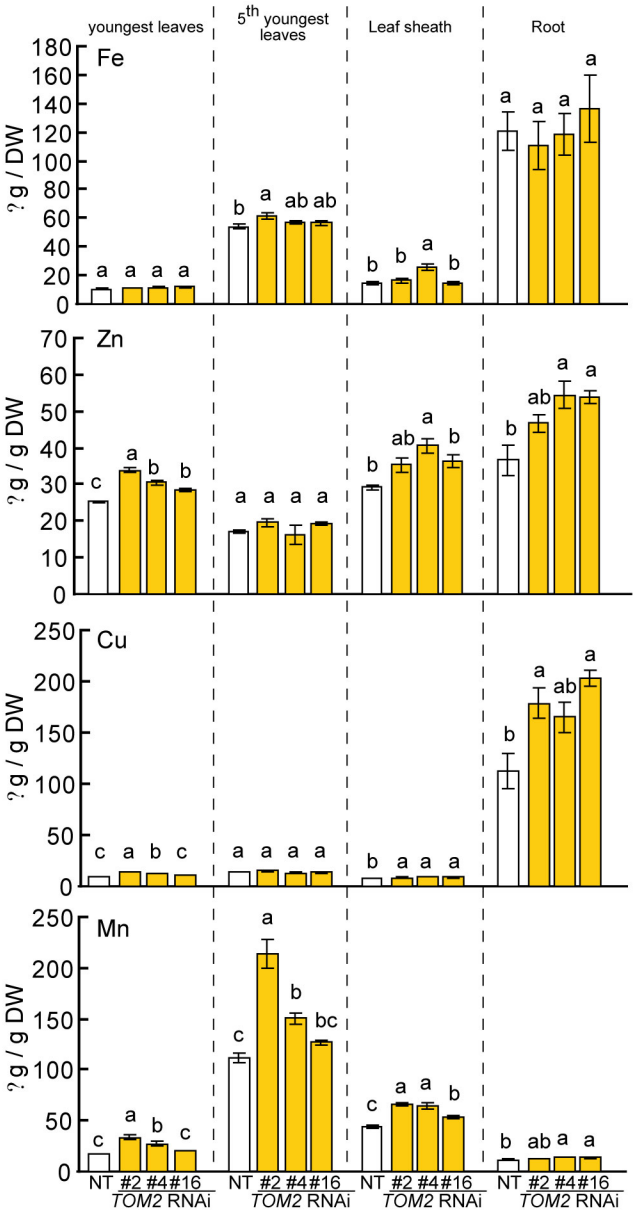

Figure 6

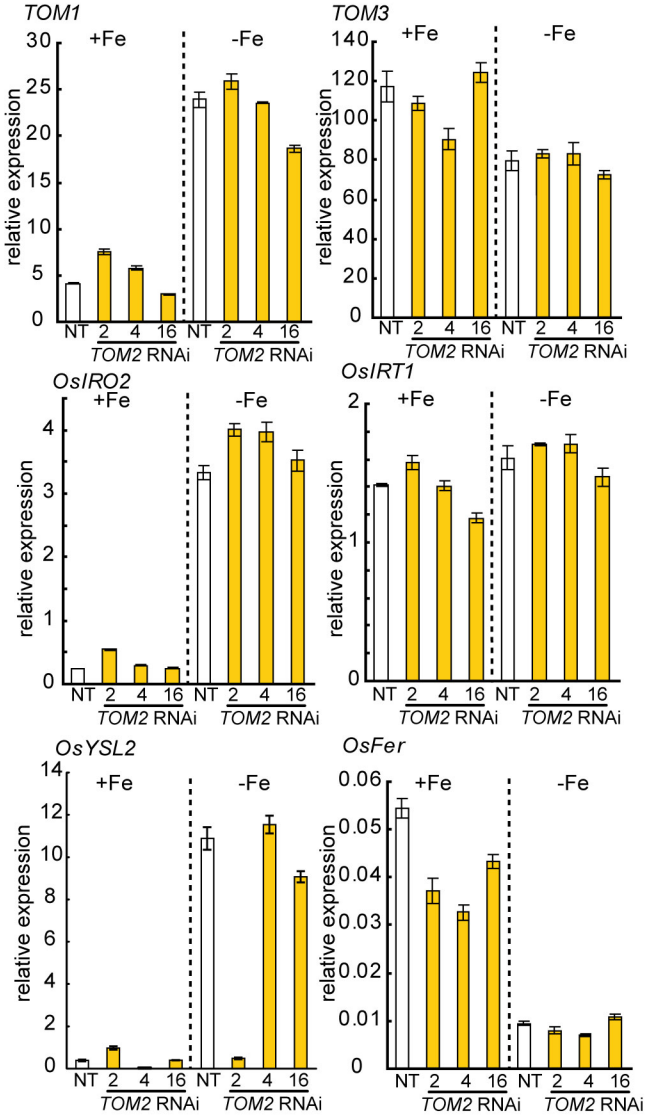

Figure 7